

Research Article

The Effect of Water Chemistry on Thermochemical Sulfate Reduction: A Case Study from the Ordovician in the Tazhong Area, Northwest China

Hongxia Li,^{1,2,3,4} Chunfang Cai,^{3,4,5} Lianqi Jia,^{3,4} Chenlu Xu,^{3,4} and Ke Zhang⁶

¹Research Institute of Unconventional Oil & Gas, Northeast Petroleum University, Daqing, Heilongjiang 163318, China

²Accumulation and Development of Unconventional Oil and Gas, State Key Laboratory Cultivation Base Jointly-Constructed by Heilongjiang Province and the Ministry of Science and Technology, Northeast Petroleum University, Daqing, Heilongjiang 163318, China

³Key Lab of Petroleum Resources Research, Institute of Geology and Geophysics, Chinese Academy of Sciences, Beijing 100029, China

⁴University of Chinese Academy of Sciences, Beijing 100049, China

⁵Key Lab of Exploration Technologies for Oil and Gas Resources of Ministry of Education, Yangtze University, Wuhan 430100, China

⁶Research Institute of Petroleum Exploration and Development, Tarim Oilfield Company, PetroChina, Korla, Xinjiang 841000, China

Correspondence should be addressed to Chunfang Cai; cai_cf@mail.iggcas.ac.cn

Received 16 February 2017; Revised 15 August 2017; Accepted 5 September 2017; Published 15 October 2017

Academic Editor: Marco Petitta

Copyright © 2017 Hongxia Li et al. This is an open access article distributed under the Creative Commons Attribution License, which permits unrestricted use, distribution, and reproduction in any medium, provided the original work is properly cited.

Formation water chemistry, sulfate sulfur isotopes, and associated H₂S contents and sulfur isotopes were measured from the Ordovician in Tazhong area, Tarim Basin. The aim is to elucidate the effects of geochemical composition of formation water on thermochemical sulfate reduction (TSR) and potential usage of SO₄/Cl ratios as a new proxy for TSR extents in areas, where H₂S and thiaadamantanes (TAs) data are not available. The formation water has SO₄/Cl ratios from 0.0002 to 0.016, significantly lower than 0.04 to 0.05 from 3 to 7 times evapoconcentrated seawater. Thus, the low values are explained to result from TSR. Furthermore, the SO₄/Cl ratios show negative correlation relationships to TAs and H₂S concentrations, indicating that TSR occurred in a relatively closed system and SO₄/Cl ratio can be used to indicate TSR extents in this area. Extensive TSR in the Cambrian in the Tazhong area, represented by low SO₄/Cl ratios and high H₂S and TAs concentrations, is accompanied by formation water with high TDS and Mg concentrations, indicating the effects of water chemistry on TSR under a realistic geological background. In contrast, the low TSR extent in the Ordovician may have resulted from limited TSR reaction duration and total contribution of aqueous SO₄²⁻.

1. Introduction

Thermochemical sulfate reduction (TSR), a process whereby aqueous sulfate and petroleum compounds react at temperatures higher than 120°C ($C_nH_{2n+2} + SO_4^{2-} \rightarrow CO_2 + H_2S + \text{altered petroleum}$), is considered to result in elevated H₂S concentrations in many carbonate reservoirs [1–8]. Significant advance has occurred on mechanisms of TSR. A great number of organic sulfides such as thiols and thiolanes [7, 9, 10] and 1- to 3-cage thiadiamondoids with 1 to 4 sulfur atoms were detected from TSR areas [11–14]. The presence of these organic sulfur compounds, especially labile sulfur compounds such as 1-pentanethiol or diethyl disulfide,

has been experimentally showed to significantly increase the rate of TSR [15]. However, hydrocarbons cannot directly react with solid sulfate in temperature from 180°C to 350°C in the laboratory [16]. Reactions between solid sulfate and gaseous hydrocarbon are quite slow even under temperatures of several hundred degrees Celsius (Kiyosu et al., 1990). Water is the solvent for chemical species and provides the aqueous matrix for all chemical reactions. Theoretical calculations by Ma et al. [17] showed that bisulfate ions (HSO₄⁻) and/or magnesium sulfate contact ion-pairs (MgSO₄ CIP) are most likely reactive sulfur species involved in TSR. Experiments indicated that the concentrations of MgSO₄ CIP are related to temperatures and SO₄/Mg ratios in the solutions [18, 19].

Consequently, water chemistry and geologic environment can strongly influence the TSR process [8, 17]. However, the effects of water chemistry on TSR are limited to theoretical and experimental studies. More researches in the real geological setting should be done.

H₂S, common in the Ordovician carbonate reservoir in the Tazhong area, is generated by TSR [20, 21]. H₂S concentration from the Ordovician in the Tazhong area is less than 10%, which is lower than that in the Khuff formation in Abu Dhabi (up to 50% [6]), the Nisku Formation in western Canada (up to 31% [22]), and the Feixianguan Formation in the northeastern Sichuan basin (up to 17% [23, 24]). The low concentrations of H₂S in the Tazhong area are considered to result from TSR process which is limited by the burial temperature [25, 26]. Besides, TSR process can be limited by water chemistry [8]. The Tazhong area is chosen as a research target and compared with the northeastern Sichuan Basin because relatively abundant information about TSR and formation water was published by previous studies. The work presented here seeks to address the following research questions: (1) what is the effect of water chemistry on TSR process and/or extent? (2) Why TSR extent in the Ordovician Yingshan Formation in the Tazhong area is low? A better understanding about the TSR mechanism will be provided through this work.

2. Geological Setting

2.1. Structural Units and Stratigraphy. Tazhong area is located in the center of Tazhong Uplift, Tarim Basin, northwest China. It is surrounded by the Manjiaer Sag, South Depression, Bachu Uplift, and Tadong Uplift (Figure 1(a)). It can be divided into number 1 Fault-slope Zone, North Slope, number 10 Structural Belt, Central Faulted Horst Belt, South Slope, and East Burial Hill Zone (Figure 1(b)). Tazhong Uplift is one of the major petroleum production areas in the Tarim Basin. Oils and natural gases have been found in the Cambrian-Ordovician carbonate reservoirs and the Silurian-Carboniferous clastic reservoirs [27].

The general stratigraphic columns of the Tazhong area were described previously [20, 25, 28, 29]. Briefly, the Cambrian strata are composed of tidal, platform, and platform-marginal carbonates. The Ordovician strata include the Upper Ordovician Sangtanmu (O_{3s}) and Lianglitage (O_{3l}) Formations and the Lower and Middle Ordovician Yingshan (O_{1-2y}) and Penglaiba (O_{1p}) Formations (Figure 2). The Lower Ordovician is predominantly composed of thick, platform facies dolomite in the lower part and limestone in the upper part. The Upper Ordovician is represented by reef and shoal facies packstone and bioclastic limestone and slope facies limestone and marlstone [9]. The Silurian to the Carboniferous sequence consists of marine sandstones and mudstones. The Permian strata are composed of lacustrine sediments and volcanic rocks. The Mesozoic and the Cenozoic are nonmarine sandstones and mudstones [20, 30, 31].

Anhydritic dolomites and anhydrite were observed in supratidal facies of the Middle Cambrian. Bedded anhydrites of 44 m~98 m thick are present in the eastern ZS1 and ZS5 wells [21]. No anhydritic carbonate was observed in the

Ordovician, which makes the geological background of TSR in the Tazhong area differentiate from the northeast Sichuan Basin.

2.2. Burial and Thermal History. TZ12 is located at the central part of number 10 Structural Belt (Figure 1(b)). Based on the burial history that rebuilt on well TZ12 (Figure 3(a)), the Lower Ordovician reached temperature of 120°C at the late Cretaceous and then reached to the maximum depth of 5000 m and temperature of 150°C at present day, whereas the Triassic Feixianguan Formation has reached temperature of 150°C since the end of the Triassic and reached temperature of 200°C at the middle Jurassic (Figure 3(b)). TSR occurred in the limestone reservoirs of the Yingshan Formation above a temperature of 120°C [20, 29].

3. Sample Collection and Analysis

A total of 17 water samples were collected from wells in the Tazhong area. These samples are used for analysis of water chemistry and S isotopic compositions of SO₄²⁻. 7 H₂S samples were collected and analyzed for S isotope. TAs concentrations in oils are obtained from previous studies.

pH was measured using an electrode method within 2 hours after sampling in the field. TDS were measured by the gravimetric method according to Clescerl et al. [32]. After filtration with a 0.45 µm filter, 0.5 ml samples of the brines were dried at 180°C until a constant weight was reached. The anions were measured by ion chromatography following appropriate dilution (5000 times for Cl and 1000 times for Br and SO₄) with a Dionex ICS900 instrument with an AS19 ion-exchange column. The analytical precisions were better than 0.8% for Cl and 4.3% for SO₄²⁻. The major cations in the diluted solutions (5000 times for all cations) were analyzed with a Varian Vista-Pro inductively coupled plasma-optical emission spectrometer (ICP-OES) with an analytical precision better than 5%.

Dissolved SO₄²⁻ was quantitatively precipitated as BaSO₄ by reacting with excess BaCl₂. This reaction was performed at a pH between 3 and 4 with HCl to prevent precipitation of BaCO₃. The precipitation of BaSO₄ was then filtered using a Buchner funnel and washed with distilled water. And then precipitation of BaSO₄ was dried and used for sulfur isotopic analysis on a Thermo Finnigan Delta S mass spectrometer. H₂S was precipitated immediately in the field by the quantitative reaction with excess zinc acetate, Zn(CH₃COO)₂, to form ZnS at a pH in the range of 10-11 (the pH was adjusted with NaOH). The solution with ZnS was put aside overnight and then filtered with a 0.45 µm filter on site. In the laboratory, ZnS was transformed to Ag₂S by adding HCl and passing the evolved H₂S under an inert atmosphere through AgNO₃ solution at a pH of 4. Ag₂S were used for sulfur isotopic analysis on a Thermo Finnigan Delta S mass spectrometer calibrated by a series of International Atomic Energy Agency standards. Results are presented as δ³⁴S relative to the Vienna Canyon Diablo Troilite (VCDT) standard. The reproducibility for δ³⁴S measurement is ±0.3‰.

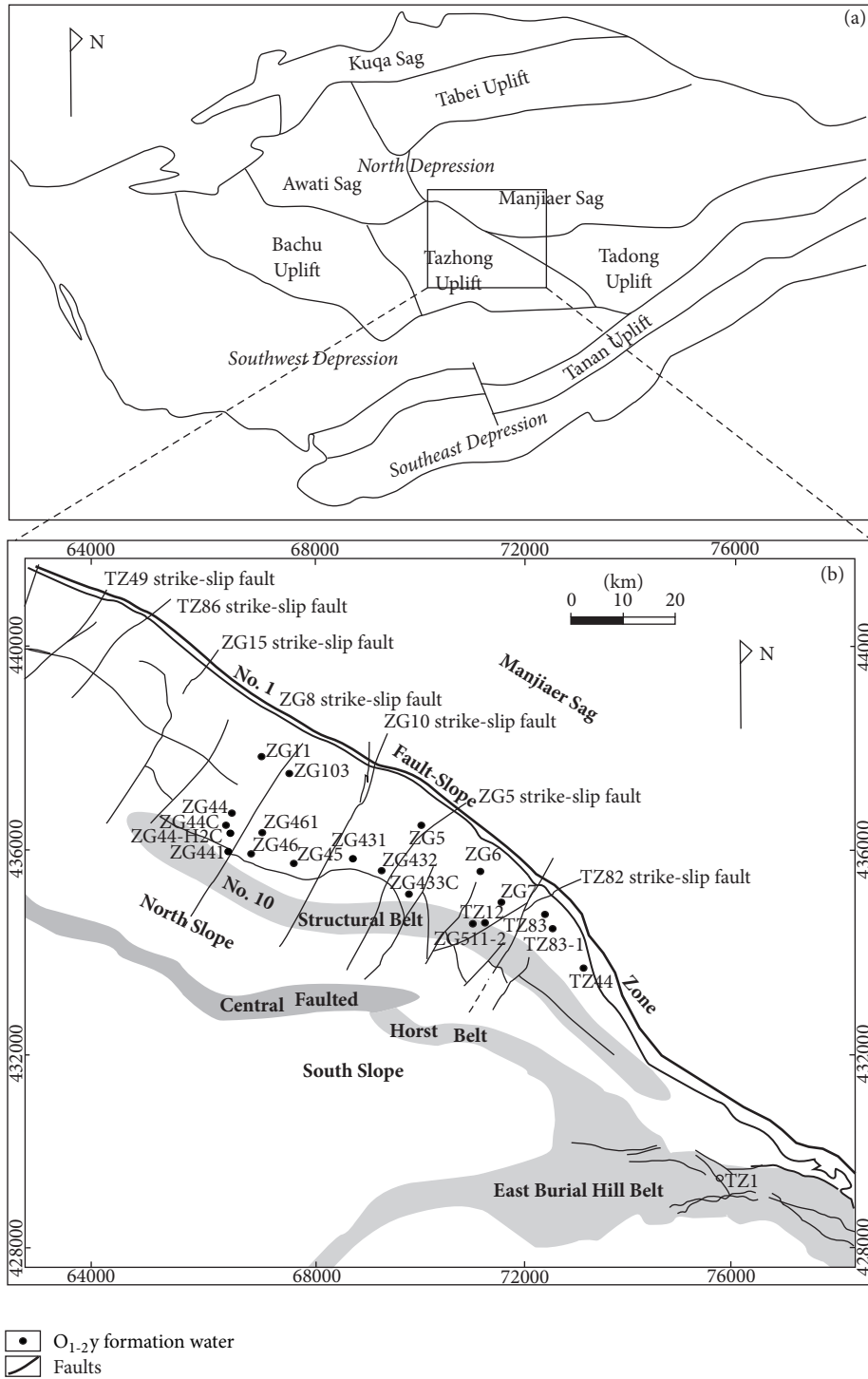


FIGURE 1: (a) Map of the Tarim Basin showing tectonic units and location of Tazhong Uplift; (b) map of the study area showing geological tectonics and location of wells from where formation waters were collected.

4. Results

4.1. Water Chemistry. Chemical compositions of formation water are shown in Table 1. The Yingshan Formation (O₁₋₂y) formation waters have Na⁺ concentrations ranging from 20140 mg/L to 64000 mg/L and Cl⁻ concentrations ranging

from 50861 mg/L to 126000 mg/L, characterized by Na/Cl molar ratios of 0.54~0.89 with an average of 0.74. The range of SO₄²⁻ concentrations is from 31 mg/L to 891 mg/L. The SO₄/Cl ratios (expressed in weight units) range from 0.0002 to 0.016 with a mean value of 0.005 (SO₄/Cl ratio of seawater is 0.144). The range of Mg²⁺ concentrations of

Strata				Lithology		Tectonic movement
Era	System	Series	Formation	Column	Description	
Paleozoic	Permian	Upper	Shajingzi		Eruptive facies tuff, basalt, and littoral mudstone	Late Hercynian
		Middle	Aqiaqun			Middle Hercynian
		Lower				
	Carboniferous	Upper	Xiaohaizi		Littoral facies sandstone and mudstone intercalate bioclastic limestone and micrite	Early Hercynian
			Kalashayi			
		Lower	Bachu			
	Devonian	Upper	Donghetang		Littoral facies sandstone and mudstone	Late Caledonian (II Phase)
		Middle-Lower				
	Silurian	Upper	Keziertage		Littoral facies sandstone and mudstone	Late Caledonian (II Phase)
		Middle	Yimugantawu			
		Lower	Tataaiertage			
			Kepingtage			
	Ordovician	Upper	Sangtamu (O _{3s})		Platform slope facies mudstone	Late Caledonian (I Phase)
			Lianglitage (O _{3l})		Platform margin facies micrite, reef limestone, and packstone	
			Tumuxiuke		Platform margin facies micrite and dolomite	
		Middle	Yijianfang		Platform margin facies micrite and dolomite	Middle Caledonian
		Lower	Yingshan (O _{1-2y})		Platform margin facies micrite and dolomite	Early Caledonian
			Penglaiba (O _{3p})		Platform facies finely dolomite and micrite	
Cambrian	Upper	Qiulitage		Platform facies finely dolomite and micrite	Early Caledonian	
		Awatage		Evaporated lagoon facies anhydritic dolomite, argillaceous dolomite		
	Middle	Shayilike		Evaporated lagoon facies anhydritic dolomite, argillaceous dolomite		
		Wusonggeer		Evaporated lagoon facies anhydritic dolomite, argillaceous dolomite		
Lower	Xiaoerbulake		Platform facies finely dolomite and interbedded mudstone			
Proterozoic	Ediacaran	Upper	Qigebulake		Platform facies finely dolomite and interbedded mudstone	Kuluketage Event
		Lower	Sugaitebulake		Terrestrial sandstone	
	Pre-Ediacaran			Tillite Granite		

FIGURE 2: Stratigraphic column for the Tazhong Uplift.

O_{1-2y} formation waters is from 92 mg/L to 1070 mg/L with an average of 638 mg/L, and the Mg/Cl ratios lie between 0.002 and 0.014 with a mean value of 0.007 (Mg/Cl ratio of seawater is 0.067). Na/Cl molar ratios of formation water are close to that of seawater (0.86). SO₄/Cl and Mg/Cl ratios of formation

water are significantly depleted compared to seawater and vary largely compared to Na/Cl molar ratios.

The Cambrian formation water has SO₄²⁻ concentration of 182 mg/L, Cl⁻ concentration of 164000 mg/L, SO₄/Cl ratio of 0.001 which is lower than most of the O_{1-2y} formation

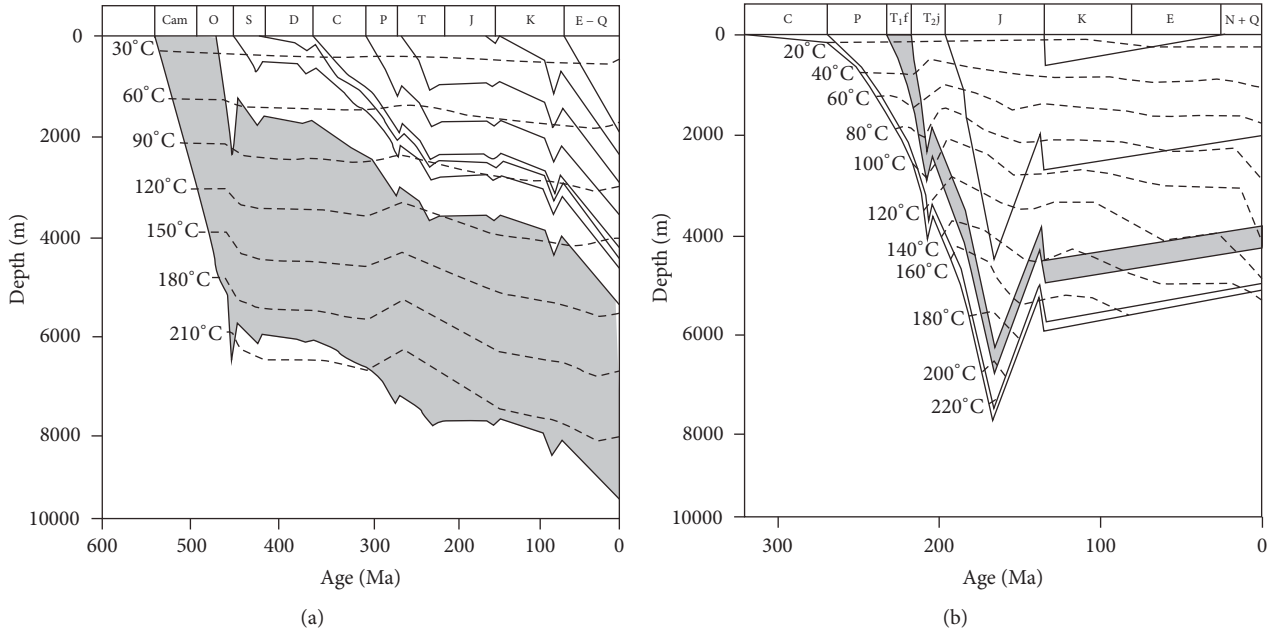


FIGURE 3: (a) Burial and paleotemperature history of the Ordovician Yingshan Formation (marked with grey color) based on the well TZ12 in the Tazhong area (modified from Chen et al., 2010). (b) Burial and paleotemperature history of the Triassic Feixianguan Formation (marked with grey color) based on the well LJ2 from the Northeast Sichuan Basin (modified from [23]).

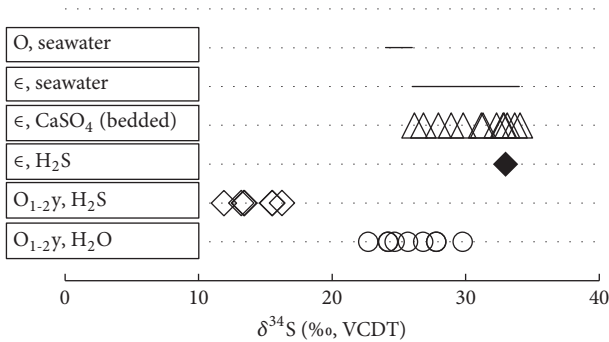


FIGURE 4: Sulfur isotopic composition of water, H₂S, and anhydrite. Sulfur isotopic of bedded anhydrite is from Cai et al. [10]. Sulfur isotopic of H₂S in the Cambrian is from Cai et al. [21].

water. The Cambrian formation water has Mg²⁺ concentration of 25500 mg/L and Mg/Cl ratios of 0.155 which is higher than that of the O₁₋₂Y formation water.

4.2. Sulfur Isotopic Composition. $\delta^{34}\text{S}_{\text{H}_2\text{S}}$ values in the O₁₋₂Y carbonate reservoir range from 11.9‰ to 16.3‰ with an average of 14.2‰ (Table 1). $\delta^{34}\text{S}$ value of H₂S from the Cambrian is 33‰ which is significantly higher than that from the O₁₋₂Y carbonate reservoir. $\delta^{34}\text{S}_{\text{SO}_4}$ values of the O₁₋₂Y formation water range from 22.7‰ to 29.8‰ with an average of 26‰ which is slightly heavier than that of coeval seawater (Figure 4). $\delta^{34}\text{S}$ values of the Cambrian bedded anhydrite lie between 26.2‰ and 33.7‰, which is similar to the Cambrian seawater. $\delta^{34}\text{S}$ values of H₂S from

the Ordovician are lighter than that of the Cambrian seawater, the Ordovician seawater, and the Cambrian bedded anhydrite (Figure 4). Sulfur isotope fractionation between SO₄ and H₂S in the Ordovician lies between 8.7‰ and 12.3‰ with an average of 10.6‰.

5. Discussion

5.1. Sulfur Isotope Composition and Fractionation. H₂S from the Ordovician carbonate reservoir in this and previous studies have $\delta^{34}\text{S}$ values from 12‰ to 16‰ which are 15‰~20‰ lighter than the counterpart in the Cambrian (33‰) [10, 21, 34]. The large differences indicate that the H₂S in the Ordovician was probably generated from in situ TSR rather than TSR that happened in the Cambrian [13, 21]. A positive relationship exists between $\delta^{34}\text{S}_{\text{H}_2\text{S}}$ values and $\delta^{34}\text{S}_{\text{SO}_4}$ values (Figure 5(a)). $\delta^{34}\text{S}_{\text{SO}_4}$ values tend to increase with a decrease of SO₄²⁻ concentrations in the formation water (Figure 5(b)). This indicates that $\delta^{34}\text{S}$ values of H₂S are related to those of the remaining SO₄²⁻. There is a positive relationship between $\delta^{34}\text{S}_{\text{SO}_4\text{-H}_2\text{S}}$ and SO₄/Cl ratios (Figure 5(c)), likely indicating that the more dissolved SO₄²⁻ is converted to H₂S, the smaller sulfur isotope fractionation occurs. This may imply that $\delta^{34}\text{S}_{\text{H}_2\text{S}}$ values are controlled by both $\delta^{34}\text{S}_{\text{SO}_4}$ values and TSR extent.

Sulfur isotope fractionation is nearly negligible if complete conversion of the available sulfate during TSR [5] (Krouse, 2001). Sulfur isotope fractionation is observed when only part of sulfate was reduced during TSR [35]. H₂S in the Cambrian carbonate reservoir has $\delta^{34}\text{S}_{\text{H}_2\text{S}}$ values close to coeval bedded anhydrite (Figure 4), whereas H₂S in the

TABLE 1: Geochemical and sulfur isotopic composition of formation water, concentrations and sulfur isotopic composition of H_2S in the gas, and concentrations of TAs in the oil in Tazhong area.

Well	Depth (m)	Strata	pH	HCO_3^- (mg/l)	Cl^- (mg/l)	SO_4^{2-} (mg/l)	Ca^{2+} (mg/l)	Mg^{2+} (mg/l)	Mg^{2+} (mg/l)	Na^+ (mg/l)	TDS (g/L)	$\delta^{34}S_{SO_4}$ (‰)	$\delta^{34}S_{H_2S}$ (‰)	H_2S (%)	TAs ($\mu g/g$)
TZ44	4873	O ₁₋₂ Y	7.0	781	50861	654	7333	92	—	84	84	—	—	0.1	32.96 [#]
TZ82	5460	O ₁₋₂ Y	6.7 [□]	778 [□]	62400 [□]	341 [□]	10500 [□]	374 [□]	—	107 [□]	107 [□]	24.7 [□]	—	0.2	—
TZ83-1	5638	O ₁₋₂ Y	6.4 ^{&}	99 ^{&}	97900 ^{&}	156 ^{&}	8741 ^{&}	684 ^{&}	51530 ^{&}	164 ^{&}	164 ^{&}	—	—	0.7	—
ZG103	6191	O ₁₋₂ Y	6.3	371	54800	321	3122	341	31970	96	96	22.7	11.9	0.4	—
ZG11	6398	O ₁₋₂ Y	6.8	527	55340	224	3240	234	—	92	92	26.8 [□]	16.3	0.6 [*]	46.63 [#]
ZG2	5880	O ₁₋₂ Y	7.1 [□]	239 [□]	58000 [□]	353 [□]	9840 [□]	395 [□]	24320 [□]	129 [□]	129 [□]	25.7 [□]	—	1.3	—
ZG433C	6133	O ₁₋₂ Y	8.0 ^{&}	484 ^{&}	120000 ^{&}	73 ^{&}	13500 ^{&}	1070 ^{&}	62400 ^{&}	204 ^{&}	204 ^{&}	—	13.2	4.9 [*]	—
ZG44	5647	O ₁₋₂ Y	7.2 ^{&}	617 ^{&}	100200 ^{&}	450 ^{&}	9635 ^{&}	770 ^{&}	53510 ^{&}	170 ^{&}	170 ^{&}	—	—	—	—
ZG44C	5647	O ₁₋₂ Y	5.5 ^{&}	3080 ^{&}	109000 ^{&}	571 ^{&}	14000 ^{&}	698 ^{&}	56900 ^{&}	188 ^{&}	188 ^{&}	—	—	—	—
ZG44-H2C	6056	O ₁₋₂ Y	6.8 ^{&}	369 ^{&}	95990 ^{&}	343 ^{&}	11150 ^{&}	768 ^{&}	46340 ^{&}	159 ^{&}	159 ^{&}	24.2	15.5 [*]	0.4 [*]	—
ZG46	5148	O ₁₋₂ Y	7.0 [□]	6358 [□]	97300 [□]	330 [□]	1580 [□]	1050 [□]	—	166 [□]	166 [□]	24.2 [□]	13.4	1.5 [*]	—
ZG461	5560	O ₁₋₂ Y	6.0	1317	56990	891	19800	810	20140	104	104	—	13.4	0.1	—
ZG5	6406	O ₁₋₂ Y	6.3 ^{&}	—	84900 ^{&}	617 ^{&}	43110 ^{&}	474 ^{&}	—	138 ^{&}	138 ^{&}	27.8	15.5	3.5 [*]	104.19 [#]
ZG511-2	5238	O ₁₋₂ Y	6.5 ^{&}	88 ^{&}	112000 ^{&}	34 ^{&}	10630 ^{&}	1003 ^{&}	52770 ^{&}	182 ^{&}	182 ^{&}	—	—	—	—
ZG6	6053	O ₁₋₂ Y	6.4 ^{&}	127 ^{&}	126000 ^{&}	31 ^{&}	13770 ^{&}	918 ^{&}	59260 ^{&}	206 ^{&}	206 ^{&}	29.8	—	7.8 [*]	147.20 [#]
ZG7	5794	O ₁₋₂ Y	7.8 [□]	871 [□]	102000 [□]	53 [□]	8890 [□]	532 [□]	—	112 [□]	112 [□]	27.8 [□]	—	4.4 [*]	100.75 [#]
ZS1C	6520	ϵ_1	6.0	274	164000	182	41300	25500	—	248	248	—	—	11 [*]	1936.6 [#]

Note that * is from Cai et al. [10], # is from Cai et al. [21], □ is Cai et al. [13], & is from Li and Cai [33], □ is from Zhang et al. [25], and “—” represents no data available.

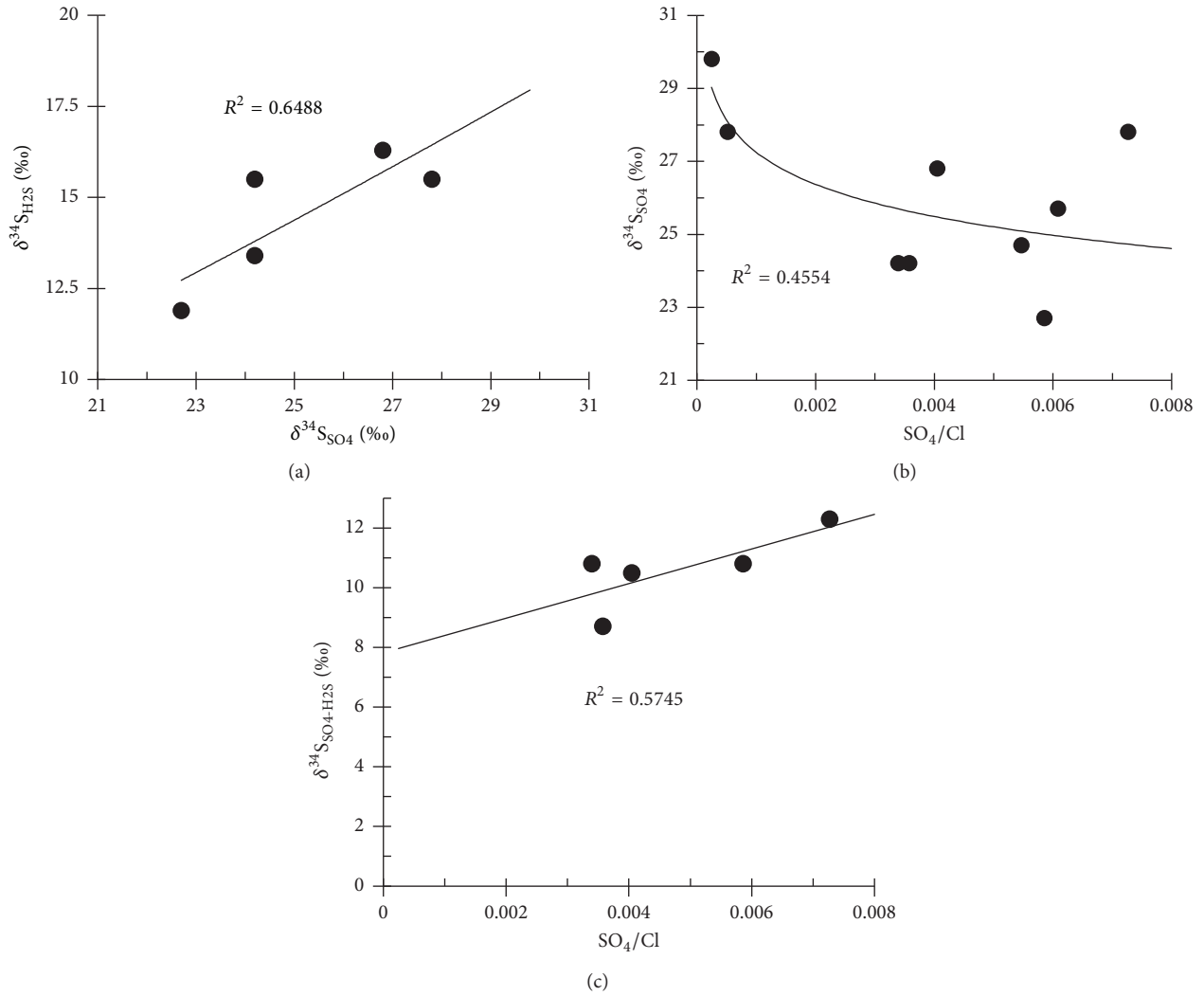


FIGURE 5: Relationship between (a) $\delta^{34}\text{S}_{\text{SO}_4}$ and $\delta^{34}\text{S}_{\text{H}_2\text{S}}$; (b) SO_4/Cl and $\delta^{34}\text{S}_{\text{SO}_4}$; (c) SO_4/Cl and $\delta^{34}\text{S}_{\text{SO}_4\text{-H}_2\text{S}}$.

Ordovician carbonate reservoir has $\delta^{34}\text{S}_{\text{H}_2\text{S}}$ values lighter than coeval seawater (22~26‰, [36]) and formation water (Figure 4). $\delta^{34}\text{S}_{\text{SO}_4\text{-H}_2\text{S}}$ differences of the Ordovician in the study area fall within a range of 8.7‰ to 12.3‰ with a mean value of 10.6‰ (Table 1). The differences of $\delta^{34}\text{S}$ values between H_2S and SO_4^{2-} in the Ordovician carbonate reservoir are higher than those of the Khuff Formation (2‰ to 3‰; [6]). This is probably due to the different geologic settings between the Abu Dhabi and the Tazhong area. TSR in the Khuff Formation of Abu Dhabi happened in the gas intervals with faster sulfate reduction than supply of reactive sulfates from anhydrite dissolution; consequently, almost all dissolved SO_4^{2-} are converted into H_2S and thus H_2S shows similar $\delta^{34}\text{S}$ values to the parent anhydrite [6]. In contrast, TSR in the Tazhong area may have happened at the oil-water transition zone [13, 14, 21]. TSR around the oil-water transition zone may have not consumed all the dissolved SO_4^{2-} ; $^{34}\text{SO}_4^{2-}$ may have been reduced preferentially as

the result of kinetic isotopic fractionation; thus, significant $\delta^{34}\text{S}_{\text{SO}_4\text{-H}_2\text{S}}$ differences are observed. Similar cases were reported from gas-water transitions in local areas from the western Canadian Basin [5] and the northeastern Sichuan Basin (Cai et al., 2010). The relatively lower H_2S concentration and higher $\delta^{34}\text{S}_{\text{SO}_4\text{-H}_2\text{S}}$ differences in the $\text{O}_{1-2}\gamma$ Formation than those in the Cambrian may indicate that only part of the dissolved SO_4^{2-} was reduced in situ in the Tazhong area, and TSR in the Ordovician is in the early stage. Zhang et al. [25] and Su et al. [26] also suggested that the overall TSR extent in the Ordovician of the Tazhong area is limited by the burial temperatures that reservoirs experienced. In other words, TSR extent is low and dissolved SO_4^{2-} is excessive for in situ TSR in the Ordovician of the Tazhong area. SO_4/Cl ratios, relating to the remaining dissolved SO_4^{2-} amounts in formation water, probably can be used as a proxy of in situ TSR extent under some circumstances, where H_2S and TAS concentrations are unavailable.

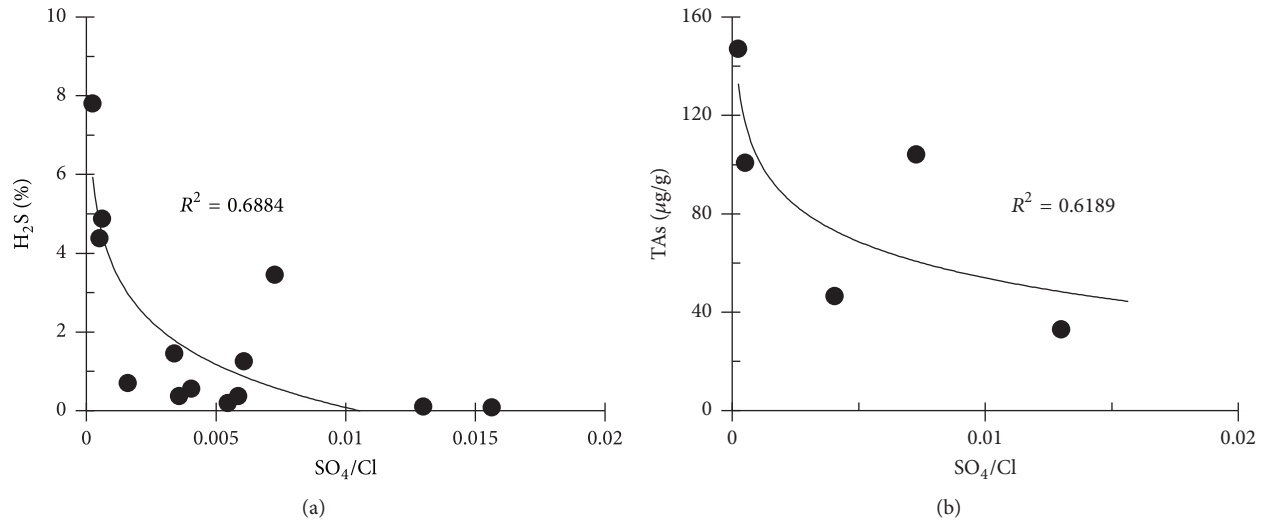


FIGURE 6: Relationship between (a) SO_4/Cl ratios and H_2S concentrations; (b) SO_4/Cl ratios and TAs concentrations.

5.2. SO_4/Cl Ratio: A Potential Proxy of TSR Extent

5.2.1. Effects of Water Evolution on SO_4/Cl Ratio. When initial seawater is evaporated and concentrated to 10 times, SO_4/Cl ratio of seawater decreases from 0.144 to 0.04 as the result of the precipitation of sulfates [37, 38]. TDS of formation water in the study area lies between 84 g/L and 206 g/L with an average of 144 g/L, which is 3 to 7 folds of seawater (35 g/L). SO_4/Cl ratios of 3 times and 7 times concentrated seawater are 0.05 and 0.04, respectively. Whereas the $\text{O}_{1-2\gamma}$ formation water has SO_4/Cl ratios from 0.0002 to 0.016, which are significantly lower than that which can be generated from the seawater evaporation. Assuming that the Cambrian to the Middle Ordovician seawater has a similar SO_4/Cl ratio, formation waters from both the Cambrian and $\text{O}_{1-2\gamma}$ evolved from evaporated seawater alone are expected to have SO_4/Cl ratios higher than 0.04; thus, it is unlikely for the mixing of evaporated formation water between the Cambrian and the $\text{O}_{1-2\gamma}$ Formation to have the low SO_4/Cl ratios (<0.016).

5.2.2. Consumption of Aqueous SO_4^{2-} by TSR. TSR is ubiquitous in the carbonate reservoirs the Tazhong area [13, 20, 21, 29, 39, 40]. TSR in the Cambrian is more extensive than that in the Ordovician, as higher H_2S concentration, higher TAs concentration, and lower SO_4/Cl ratio were observed (Table 1). TSR consumes dissolved SO_4^{2-} , leading to lower SO_4/Cl ratios in the formation water than original seawater. The depletion of SO_4^{2-} in the $\text{O}_{1-2\gamma}$ formation water was not compensated by anhydrite dissolution as no anhydrite or anhydritic carbonate rocks develop in the Ordovician strata (Figure 2).

H_2S , a direct product of TSR, can dissolve in formation water, precipitate as pyrite, and be incorporated into oils and solid bitumens producing alkylthiolanes, alkylthiols, and alkyl 2-thiaadamantanes [7, 13, 21]. Thiaadamantanes (TAs) concentrations in petroleum are considered to better reflect TSR extents because TAs is quite stable even under high

temperature [13, 14, 41]. However, TAs concentrations are only measured in several wells. Negative relationships exist in SO_4/Cl ratios versus H_2S concentrations and SO_4/Cl ratios versus TAs concentrations (Figures 6(a) and 6(b)). This indicates that SO_4^{2-} was transformed to H_2S by TSR and subsequently to incorporate into TAs in a relatively closed system. Thus, SO_4/Cl ratio is expected to be a good proxy to reflect TSR extent if they are not significantly changed by water mixing or anhydrite dissolution.

5.3. Influence of Water Chemistry on TSR Initiation. TSR is commonly observed in carbonate reservoirs with high-temperature, but it is difficult to repeat the TSR process in the laboratory under conditions resembling nature. Dissolved SO_4^{2-} , with symmetrical molecular structure and spherical electronic distributions, have extremely low reactivity in the absence of catalysis [17]. TSR reactions that occur in natural environments are most likely to involve magnesium sulfate (MgSO_4) rather than “free” dissolved sulfate ions (SO_4^{2-}) or solvated sulfate ion-pairs. MgSO_4 has been proved to be an effective catalysis for TSR in the laboratory [17, 42]. MgSO_4 exists as a main magnesium-bearing specie in solutions with Mg^{2+} being dominant [43]. As temperature increases, MgSO_4 solutions were separated into MgSO_4 -rich phase and MgSO_4 -poor phase due to the formation of the complex $\text{Mg}^{2+}\text{-SO}_4^{2-}$ ion association in the fused silica capillary capsules, and the phase separation temperature decreases with increasing Mg/SO_4 ratios [19]. This indicates that formation water with high Mg concentrations and high temperature is preferable to form MgSO_4 and initiate TSR.

Figures 7(a), 7(b), and 7(c) show a negative relationship between Mg concentrations and SO_4/Cl ratios, a positive relationship between Mg concentrations and H_2S concentrations, and a positive relationship between Mg concentrations and TAs concentrations. This indicates that the TSR extent is high in formation water with high Mg concentrations, which

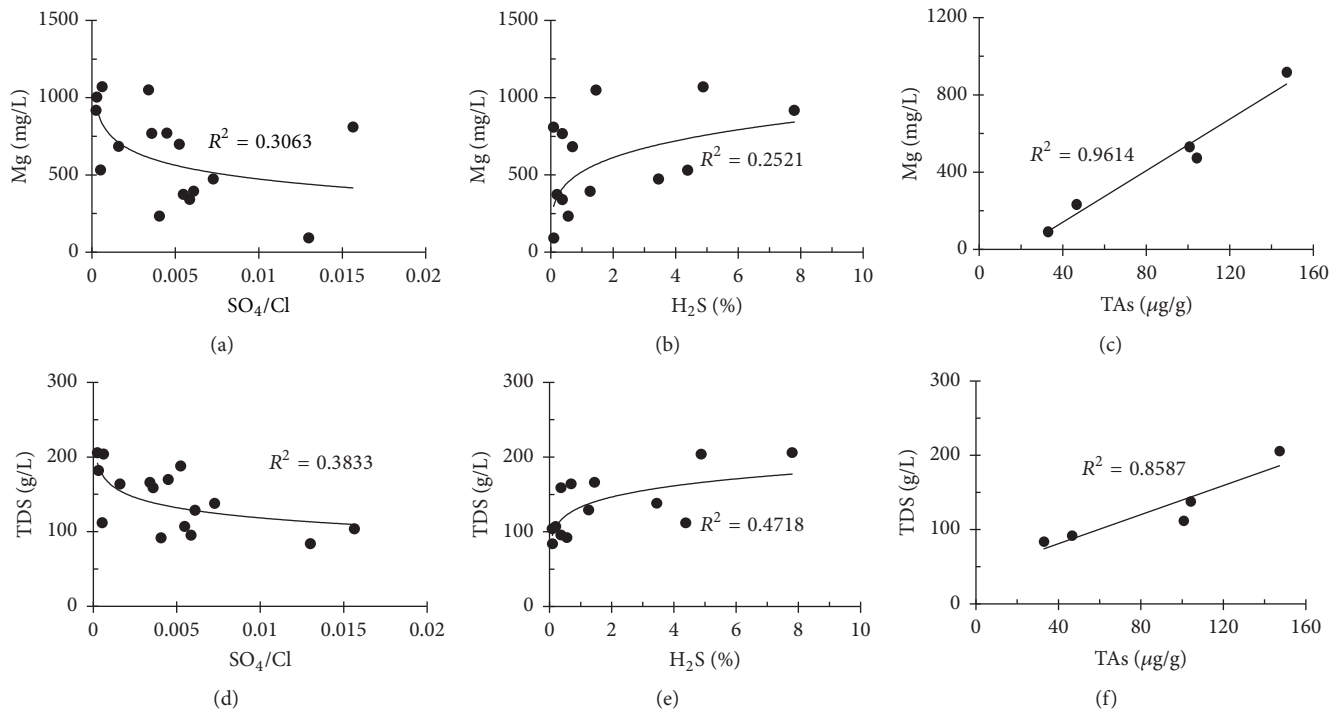


FIGURE 7: Relationship between (a) SO_4/Cl ratios and Mg concentrations; (b) H_2S concentrations and Mg concentrations; (c) TAs concentrations and Mg concentrations; (d) SO_4/Cl ratios and TDS; (e) H_2S concentrations and TDS; (f) TAs concentrations and TDS.

prove the catalysis of MgSO_4 . TDS concentrations show a negative correlation with SO_4/Cl ratios, a positive correlation with H_2S concentrations, and a positive correlation with TAs concentrations (Figures 7(d), 7(e), and 7(f)). This also indicates the catalysis of MgSO_4 as Mg concentration is in proportion to TDS in this study.

Mean Mg/Cl ratios in the formation water from the Yingshan Formation is 0.007, which is similar to that from the Feixianguan Formation (0.009 [44]). But average Mg/ SO_4 ratio in the formation water from the Yingshan Formation is 6.24, which is significantly higher than that from the Feixianguan Formation (0.035 [44]). The low Mg/ SO_4 ratios in the formation water from the Feixianguan Formation resulted from the high SO_4 concentration contributed by anhydrite dissolution. The limitation on TSR initiation from low Mg/ SO_4 ratios in the Feixianguan Formation was probably compensated by the high temperature in the reservoir (Figure 3(b)). Similarly, the limitation on TSR initiation from low temperature in the Yingshan Formation was compensated by the high Mg/ SO_4 ratios in the formation water. Duration time of TSR in the Feixianguan Formation is much longer than that in the Yingshan Formation as temperature of the Feixianguan Formation has reached 200°C since the Middle Jurassic (Figure 3(b)). And reaction rate of TSR in the Feixianguan Formation is also faster than that in the Yingshan Formation. Moreover, contribution of total aqueous SO_4^{2-} in the Feixianguan Formation is more than that in the Yingshan Formation as many anhydrites develop in the Feixianguan Formation. These are probably the main reasons for the lower H_2S concentrations in the Tazhong area than that in the northeast Sichuan Basin.

6. Conclusions

Formation water is the solvent for sulfates, and water chemistry has a great influence on TSR which explain the low TSR extent in the Tazhong area.

(1) MgSO_4 contact ion pair in formation water is catalyst for TSR. High Mg/ SO_4 ratios and high temperatures are preferable to form MgSO_4 contact ion pair in solutions and thus will increase TSR extent. High Mg/ SO_4 ratios of the $\text{O}_{1-2}\gamma$ formation water compensated the low temperature which would limit the initiation of TSR in the Tazhong area.

(2) The lower TSR extent in the Tazhong area is limited by the shorter reaction time and less total aqueous SO_4^{2-} contribution in the reservoir.

Conflicts of Interest

The authors declare that there are no conflicts of interest regarding the publication of this paper.

Acknowledgments

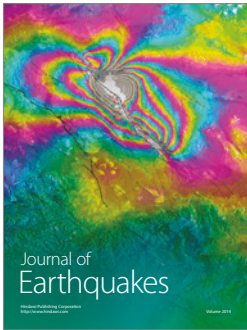
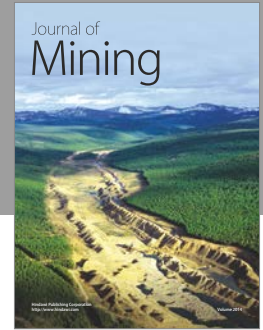
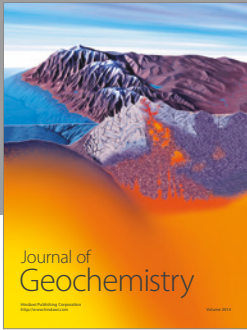
This work is supported by the Natural Science Foundation of China (Grants nos. 41672143, 41730424, and 41502148) and Special Major Project on Petroleum Study (2017ZX05008003-040).

References

- [1] W. L. Orrm, "Changes in sulfur content and isotopic ratios of sulfur during petroleum maturation—study of the Big Horn

- Basin Paleozoic oils," *AAPG Bulletin*, vol. 50, pp. 2295–2318, 1974.
- [2] H. R. Krouse, C. A. Viau, L. S. Eliuk, A. Ueda, and S. Halas, "Chemical and isotopic evidence of thermochemical sulphate reduction by light hydrocarbon gases in deep carbonate reservoirs," *Nature*, vol. 333, no. 6172, pp. 415–419, 1988.
 - [3] R. Sassen, "Geochemical and carbon isotopic studies of crude oil destruction, bitumen precipitation, and sulfate reduction in the deep Smackover Formation," *Organic Geochemistry*, vol. 12, no. 4, pp. 351–361, 1988.
 - [4] E. Heydari, C. H. Moore, and R. Sassen, "Late burial diagenesis driven by thermal-degradation of hydrocarbons and thermochemical sulfate reduction—upper Smackover carbonates, southeast Mississippi salt basin," *AAPG Bulletin*, vol. 72, p. 197, 1988.
 - [5] H. G. Machel, H. R. Krouse, and R. Sassen, "Products and distinguishing criteria of bacterial and thermochemical sulfate reduction," *Applied Geochemistry*, vol. 10, no. 4, pp. 373–389, 1995.
 - [6] R. H. Worden and P. C. Smalley, "H₂S-producing reactions in deep carbonate gas reservoirs: Khuff Formation, Abu Dhabi," *Chemical Geology*, vol. 133, no. 1–4, pp. 157–171, 1996.
 - [7] C. F. Cai, R. H. Worden, S. H. Bottrell, L. Wang, and C. Yang, "Thermochemical sulphate reduction and the generation of hydrogen sulphide and thiols (mercaptans) in Triassic carbonate reservoirs from the Sichuan Basin, China," *Chemical Geology*, vol. 202, no. 1–2, pp. 39–57, 2003.
 - [8] Y. J. Fu, W. van Berk, and H. M. Schulz, "Hydrogen sulfide formation, fate, and behavior in anhydrite-sealed carbonate gas reservoirs: a three-dimensional reactive mass transport modeling approach," *AAPG Bulletin*, vol. 100, no. 5, pp. 843–865, 2016.
 - [9] C. F. Cai, K. Li, M. Anlai et al., "Distinguishing Cambrian from Upper Ordovician source rocks: Evidence from sulfur isotopes and biomarkers in the Tarim Basin," *Organic Geochemistry*, vol. 40, no. 7, pp. 755–768, 2009.
 - [10] C. F. Cai, C. Zhang, L. Cai et al., "Origins of Palaeozoic oils in the Tarim Basin: Evidence from sulfur isotopes and biomarkers," *Chemical Geology*, vol. 268, no. 3–4, pp. 197–210, 2009.
 - [11] S. Hanin, P. Adam, I. Kowalewski, A.-Y. Huc, B. Carpentier, and P. Albrecht, "Bridgehead alkylated 2-thiaadamantanes: Novel markers for sulfurisation processes occurring under high thermal stress in deep petroleum reservoirs," *Chemical Communications*, vol. 16, pp. 1750–1751, 2002.
 - [12] Z. Wei, P. Mankiewicz, C. Walters et al., "Natural occurrence of higher thiadiamondoids and diamondoidthiols in a deep petroleum reservoir in the Mobile Bay gas field," *Organic Geochemistry*, vol. 42, no. 2, pp. 121–133, 2011.
 - [13] C. F. Cai, A. Amrani, R. H. Worden et al., "Sulfur isotopic compositions of individual organosulfur compounds and their genetic links in the Lower Paleozoic petroleum pools of the Tarim Basin, NW China," *Geochimica et Cosmochimica Acta*, vol. 182, pp. 88–108, 2016.
 - [14] C. F. Cai, Q. Xiao, C. Fang, T. Wang, W. He, and H. Li, "The effect of thermochemical sulfate reduction on formation and isomerization of thiadiamondoids and diamondoids in the Lower Paleozoic petroleum pools of the Tarim Basin, NW China," *Organic Geochemistry*, vol. 101, pp. 49–62, 2016.
 - [15] A. Amrani, T. Zhang, Q. Ma, G. S. Ellis, and Y. Tang, "The role of labile sulfur compounds in thermochemical sulfate reduction," *Geochimica et Cosmochimica Acta*, vol. 72, no. 12, pp. 2960–2972, 2008.
 - [16] W. G. Toland, "Oxidation of organic compounds with aqueous sulfate," *Journal of the American Chemical Society*, vol. 82, no. 8, pp. 1911–1916, 1960.
 - [17] Q. Ma, G. S. Ellis, A. Amrani, T. Zhang, and Y. Tang, "Theoretical study on the reactivity of sulfate species with hydrocarbons," *Geochimica et Cosmochimica Acta*, vol. 72, no. 18, pp. 4565–4576, 2008.
 - [18] X. Wang, I.-M. Chou, W. Hu, and R. C. Burruss, "In situ observations of liquid-liquid phase separation in aqueous MgSO₄ solutions: geological and geochemical implications," *Geochimica et Cosmochimica Acta*, vol. 103, pp. 1–10, 2013.
 - [19] Y. Wan, X. L. Wang, W. X. Hu, and I.-M. Chou, "Raman spectroscopic observations of the ion association between Mg²⁺ and SO₄²⁻ in MgSO₄-saturated droplets at temperatures of ≤380°C," *The Journal of Physical Chemistry A*, vol. 119, no. 34, pp. 9027–9036, 2015.
 - [20] C. F. Cai, W. Hu, and R. H. Worden, "Thermochemical sulphate reduction in Cambro-Ordovician carbonates in Central Tarim," *Marine and Petroleum Geology*, vol. 18, no. 6, pp. 729–741, 2001.
 - [21] C. F. Cai, G. Y. Hu, H. X. Li et al., "Origins and fates of H₂S in the Cambrian and Ordovician in Tazhong area: evidence from sulfur isotopes, fluid inclusions and production data," *Marine and Petroleum Geology*, vol. 67, pp. 408–418, 2015.
 - [22] B. K. Manzano, M. G. Fowler, and H. G. Machel, "The influence of thermochemical sulphate reduction on hydrocarbon composition in Nisku reservoirs, Brazeau river area, Alberta, Canada," *Organic Geochemistry*, vol. 27, no. 7–8, pp. 507–521, 1997.
 - [23] C. F. Cai, Z. Xie, R. H. Worden, G. Hu, L. Wang, and H. He, "Methane-dominated thermochemical sulphate reduction in the Triassic Feixianguan Formation East Sichuan Basin, China: Towards prediction of fatal H₂S concentrations," *Marine and Petroleum Geology*, vol. 21, no. 10, pp. 1265–1279, 2004.
 - [24] G. Y. Zhu, J. F. Chen, G. A. Fei, J. Zhao, and C. Liu, "Sulfur isotopic fractionation and mechanism for Thermochemical Sulfate Reduction genetic H₂S," *Acta Petrologica Sinica*, vol. 30, no. 12, pp. 3772–3778, 2014.
 - [25] S. Zhang, J. Su, H. Huang et al., "Genetic origin of sour gas condensates in the Paleozoic dolomite reservoirs of the Tazhong Uplift, Tarim Basin," *Marine and Petroleum Geology*, vol. 68, pp. 107–119, 2015.
 - [26] J. Su, S. C. Zhang, H. P. Huang et al., "New insights into the formation mechanism of high hydrogen sulfide-bearing gas condensates: case study of Lower Ordovician dolomite reservoirs in the Tazhong uplift, Tarim Basin," *AAPG Bulletin*, vol. 100, no. 6, pp. 893–916, 2016.
 - [27] X.-X. Lu, Z.-J. Jin, L.-F. Liu et al., "Oil and gas accumulations in the Ordovician carbonates in the Tazhong Uplift of Tarim Basin, west China," *Journal of Petroleum Science and Engineering*, vol. 41, no. 1–3, pp. 109–121, 2004.
 - [28] C. F. Cai, S. G. Franks, and P. Aagaard, "Origin and migration of brines from Paleozoic strata in Central Tarim, China: constraints from ⁸⁷Sr/⁸⁶Sr, δd, δ¹⁸O and water chemistry," *Applied Geochemistry*, vol. 16, no. 9–10, pp. 1269–1284, 2001.
 - [29] L. Jia, C. Cai, H. Yang et al., "Thermochemical and bacterial sulfate reduction in the Cambrian and Lower Ordovician carbonates in the Tazhong Area, Tarim Basin, NW China: Evidence from fluid inclusions, C, S, and Sr isotopic data," *Geofluids*, vol. 15, no. 3, pp. 421–437, 2015.

- [30] Z. Q. Chen and G. R. Shi, "Late paleozoic depositional history of the Tarim basin, northwest China: An integration of biostratigraphic and lithostratigraphic constraints," *AAPG Bulletin*, vol. 87, no. 8, pp. 1323–1354, 2003.
- [31] H. Pang, J. Q. Chen, X. Q. Pang, K. Y. Liu, and C. F. Xiang, "Estimation of the hydrocarbon loss through major tectonic events in the Tazhong area, Tarim Basin, west China," *Marine and Petroleum Geology*, vol. 38, no. 1, pp. 195–210, 2012.
- [32] L. S. Clescerl, A. E. Greenberg, and A. D. Eaton, *Standard Methods for the Examination of Water and Wastewater*, American Public Health Association, Washington, DC, USA, 20th edition, 1999.
- [33] H. Li and C. F. Cai, "Origin and evolution of formation water from the Ordovician carbonate reservoir in the Tazhong area, Tarim Basin, NW China," *Journal of Petroleum Science and Engineering*, vol. 148, pp. 103–114, 2017.
- [34] C. F. Cai, K. Li, H. Li, and B. Zhang, "Evidence for cross formational hot brine flow from integrated $^{87}\text{Sr}/^{86}\text{Sr}$, REE and fluid inclusions of the Ordovician veins in Central Tarim, China," *Applied Geochemistry*, vol. 23, no. 8, pp. 2226–2235, 2008.
- [35] J. G. Wynn, J. B. Sumrall, and B. P. Onac, "Sulfur isotopic composition and the source of dissolved sulfur species in thermo-mineral springs of the Cerna Valley, Romania," *Chemical Geology*, vol. 271, no. 1-2, pp. 31–43, 2010.
- [36] G. E. Claypool and E. A. Mancini, "Geochemical relationships of petroleum in Mesozoic reservoirs to carbonate source rocks of Jurassic Smackover Formation, southwestern Alabama," *American Association of Petroleum Geologists Bulletin*, vol. 73, no. 7, pp. 904–924, 1989.
- [37] M. A. McCaffrey, B. Lazar, and Holland, "The evaporation path of seawater and the coprecipitation of Br^- and K^+ with halite," *Journal of Sedimentary Petrology*, vol. 57, no. 5, pp. 928–937, 1987.
- [38] B. W. Logan, "The Mac Leod evaporite basin, western Australia. Holocene environments, sediments and geological evolution," *AAPG Memoir*, vol. 44, pp. 1–140, 1987.
- [39] Z. Wang, C. Cai, H. Li et al., "Origin of late charged gas and its effect on property of oils in the Ordovician in Tazhong area," *Journal of Petroleum Science and Engineering*, vol. 122, pp. 83–93, 2014.
- [40] K. Li, C. Cai, L. Jia et al., "The role of thermochemical sulfate reduction in the genesis of high-quality deep marine reservoirs within the central Tarim Basin, western China," *Arabian Journal of Geosciences*, vol. 8, no. 7, pp. 4443–4456, 2015.
- [41] Z. Wei, C. C. Walters, J. Michael Moldowan et al., "Thiadiazonoids as proxies for the extent of thermochemical sulfate reduction," *Organic Geochemistry*, vol. 44, pp. 53–70, 2012.
- [42] S. C. Zhang, Y. H. Shuai, K. He, and J. K. Mi, "Research on the initiation mechanism of thermochemical sulfate reduction (TSR)," *Acta Petrologica Sinica*, vol. 28, no. 3, pp. 739–748, 2012.
- [43] M. Baghalha and V. G. Papangelakis, "The ion-association-interaction approach as applied to aqueous $\text{H}_2\text{SO}_4\text{-Al}_2(\text{SO}_4)_3\text{-MgSO}_4$ solutions at 250°C," *Metallurgical and Materials Transactions B*, vol. 29, no. 5, pp. 1021–1030, 1998.
- [44] X. Q. Zhao, J. F. Chen, W. Guo, D. X. He, F. R. Chen, and G. Z. Liu, "Geochemical characteristics of oilfield waters with high H_2S gas reservoirs in Feixianguan formation, Northeastern Sichuan Basin," *Journal of Central South University (Science and Technology)*, vol. 45, no. 10, pp. 300–309, 2014.



Hindawi

Submit your manuscripts at
<https://www.hindawi.com>

